Draft chapter last generated 2024-12-02; P.H. Trinh

13

History: see original paper in Saffman and Taylor [1958] and eventual resolution Combescot et al. [1986, 1988], Combescot and Dombre [1988], Hong and Langer [1986, 1987]. More modern treatments using exponential asymptotics in Tanveer [1990], Chapman [1999].

13.1 THE SAFFMAN-TAYLOR PROBLEM

We first describe the experiment and findings in the original paper by Saffman and Taylor [1958]. A Hele-Shaw cell is constructed using two pieces of glass separated by a thin gap filled with viscous fluid (glycerine). A pressure gradient is produced by applying air pressure or suction above the fluid in one end of the apparatus, while the other end is maintained at atmospheric pressure. This apparatus appears in fig. 13.1.

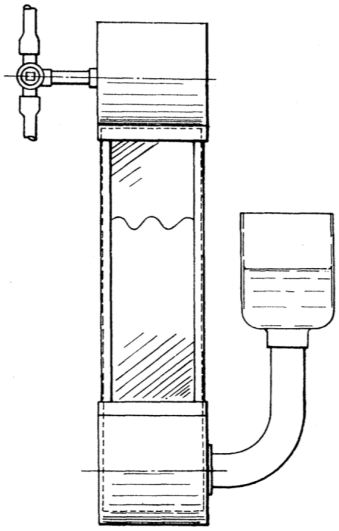

Figure 13.1: Sketch of a Hele-Shaw cell. Figure from Saffman and Taylor [1958].

When the pressure gradient is applied, the air-liquid interface is observed to destabilise in a process known as *viscous fingering*. Here, the initial, nearly straight interface develops oscillatory instabilities that eventually grow into longer 'fingers' of bubbles, as shown in fig. 13.2. The experiment can be repeated by injecting a less viscous fluid into a more viscous fluid and the instability also appears.

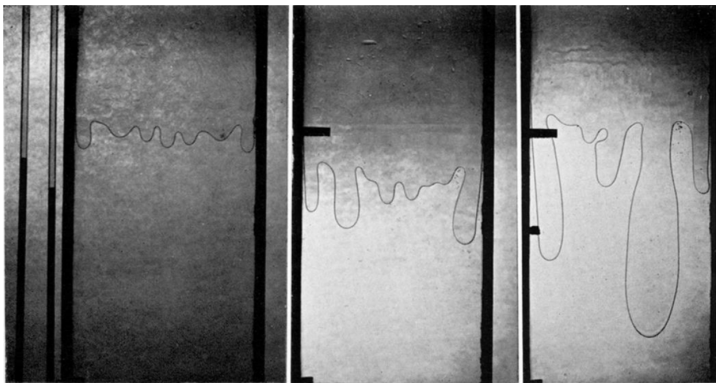

Figure 13.2: Sketch of a Hele-Shaw cell (from Saffman and Taylor 1958)

Saffman and Taylor [1958] argued that one could model the situation by considering the case of an infinite set of equal and equally spaced fingers all advancing at the same speed. Since each finger is then separated with its neighbour by a streamline, one is led to consider the simplest scenario of single finger propagating, in a Hele-Shaw channel of fixed width.

Let us explain the connection with exponential asymptotics. The non-dimensional parameter that appears in the mathematical model is the inverse-capillary number

$$\epsilon^2 \propto \frac{\sigma}{\mu U(1-\lambda)^2}, \tag{13.1}$$

where μ is the dynamic viscosity of the liquid, U is the speed of the travelling finger, σ is the surface tension, and $0 < \lambda < 1$ is the proportion of the (transverse) channel width that is occupied by the finger.

Through a procedure of conformal mapping and seeking the limit of $\epsilon \to 0$, Saffman and Taylor demonstrated that a leading-order approximation could be developed for the finger profile [their eqn (17)],

$$x \sim \frac{1-\lambda}{\pi} \log\left[\frac{1}{2}\left(1 + \cos\frac{\pi y}{\lambda}\right)\right], \tag{13.2}$$

for a bubble propagating in the positive x direction with the tip of the bubble at $(x, y) = (0, 0)$. Note that the approximation yields a finger profile for different widths λ. Figure 13.3 demonstrates the remarkable fit between experiment and their asymptotic approximation.

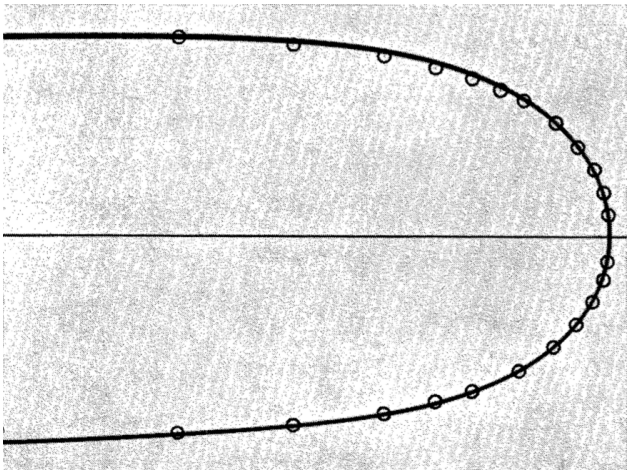

Figure 13.3: Fit between theory and experiment (from figure 9, plate 2 of Saffman and Taylor 1958)

However, Saffman and Taylor crucially remarked that [p. 327]

> *"The most interesting feature of the results exhibited... is that in all cases the value of λ rapidly decreases as [the Capillary number] increases till it reaches a value which is very close to $\frac{1}{2}$... We have found no theoretical reason for this deduction."*

Thus the asymptotic approximation (13.2) seems to yield no restriction on the permissible values of λ in the limit $\epsilon \to 0$ and a one-parameter family of solutions is predicted—in seeming contradiction with the experimental results.

The selection mechanism that determines the permissible values of ϵ will turn out to be an exponential asymptotics problem.

13.2 MATHEMATICAL FORMULATION

This formulation follows McLean and Saffman [1981], Vanden-Broeck [2010], Chapman [1999]. Consider a Hele-Shaw cell composed of a long and thin rectilinear channel of dimensional width $2a$ and height b, where $b \ll a$. The cell is filled with an incompressible fluid of viscosity μ that is pushed by a non-miscible second fluid of negligible viscosity. Gravity is ignored. We suppose that a travelling wave has formed in which a

single finger of the inviscid fluid with width $2\lambda a$ as $x \to -\infty$ propogates at velocity U.

A derivation of the governing mathematical model is presented in **??**, and here we present only the key details. The system is firstly non-dimensionalised: the lengths are non-dimensionalised with a, velocity with $(1-\lambda)U$, and pressure with $12\mu a(1-\lambda)U/b^2$. Once this is done, a velocity potential ϕ is introduced for the coordinate frame moving with the finger. The task is to solve Laplace's equation, $\nabla^2\phi = 0$, within the viscous fluid subject to kinematic conditions on all solid and free boundaries. In addition, on the free surface, we impose the dynamic condition,

$$\phi = \phi_0 + C\kappa - \frac{x}{1-\lambda},$$

where ϕ_0 is the constant value of the potential in the inviscid region, κ is the non-dimensional curvature of the interface, and

$$C = \frac{\sigma b^2}{12\mu a^2 U(1-\lambda)},$$

is the inverse Capillary number. Finally, for the viscous fluid outside of the bubble, we require the two far-field conditions of

$$\begin{aligned} &\phi_x \sim -1/(1-\lambda) && \text{as } x \to -\infty,\ \lambda < |y| < 1, \\ &\phi_x \sim -1 && \text{as } x \to +\infty,\ -1 < y < 1, \end{aligned}$$

which imposes, respectively, the fluid speeds far behind and far ahead of the finger tip.

The problem is now reformulated with the help of complex-variable theory. First, a series of conformal maps are applied that transforms the physical flow domain into a simpler domain. And second, Cauchy's theorem is applied in order to repose the problem as a one-dimensional boundary integral formulation. This essentially side-steps the issue of having to solve Laplace's equation in a fully two-dimensional region with unknown boundaries.

Consider a point, $z = x + \mathrm{i}y$, on the interface, as shown in fig. 13.4. We let $w = \phi + \mathrm{i}\psi$ be the complex potential. The fluid region in the z-plane is now mapped to a strip region in the w-plane. We further set

$$s = \mathrm{e}^{-(w-\phi_0)\pi}, \tag{13.3}$$

which maps the fluid region to the upper-half s-plane, where the interface AB is mapped to the real segment $0 < s < 1$ with $s = 1$ corresponding to the finger tip. The s-plane is shown in fig. 13.5.

Let $\hat{q}$ and $\hat{\theta}$ be respectively the non-dimensional speed and angle of the interface, measured relative to the positive x-axis. Then, the complex velocity can be written as

$$u - \mathrm{i}v = \hat{q}\mathrm{e}^{-\mathrm{i}\hat{\theta}}.$$

Next, we shift the angle and scale the speed using

$$\theta = \hat{\theta} - \pi, \qquad q = (1-\lambda)\hat{q},$$

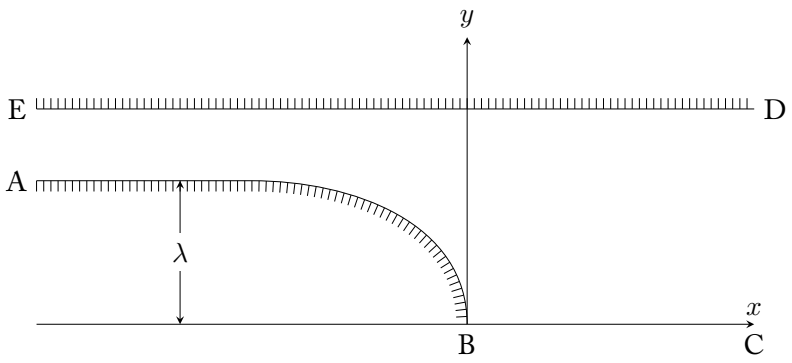

Figure 13.4: Configuration in the z-plane.

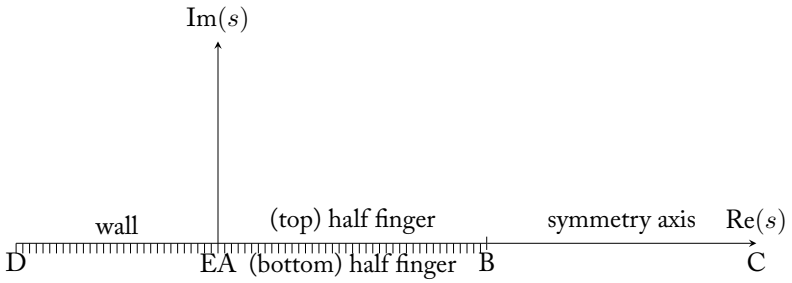

Figure 13.5: Configuration in the s-plane. Note that the finger has been mapped to the region $0 < s < 1$.

which will have the effect of simplifying the governing equations and moving the only appearance of the finger width, λ, to a single combined parameter.

It can then be shown that solving the steady viscous fingering problem is equivalent to obtaining functions, $q = q(s)$ and $\theta = \theta(s)$, such that

$$\log q = -\frac{s}{\pi}\fint_0^1 \frac{\theta(s')}{s'(s'-s)}\,\mathrm{d}s' \tag{13.4a}$$

$$\epsilon^2 qs\frac{\mathrm{d}}{\mathrm{d}s}\left(qs\frac{\mathrm{d}\theta}{\mathrm{d}s}\right) - q = -\cos\theta \tag{13.4b}$$

$$\theta(0) = 0, \qquad q(0) = 1 \tag{13.4c}$$

$$\theta(1) = -\frac{\pi}{2}, \qquad q(1) = 0, \tag{13.4d}$$

which is to be solved on the strip $0 \le s \le 1$. The above system is the McLean and Saffman [1981] formulation. See also eqns (2.15)–(2.19) from Chapman [1999]. The small parameter that has been introduced is the dimensionless surface tension,

$$\epsilon^2 = \frac{C\pi^2}{1-\lambda} = \frac{\sigma b^2\pi^2}{12\mu U a^2(1-\lambda)^2}. \tag{13.5}$$

Once the system (13.4) has been solved, we can retrieve the shape of the finger by computing

See Vanden-Broeck [2010] eqn (3.270).

$$x(s) + \mathrm{i}y(s) = -\frac{1-\lambda}{\pi}\int_s^1 \frac{\mathrm{e}^{\mathrm{i}\theta(s')}}{s'q(s')}\,\mathrm{d}s', \tag{13.6}$$

and furthermore the width can be calculated from

$$\log(1-\lambda) = \frac{1}{\pi}\fint_0^1 \frac{\theta(s')}{s'}\,\mathrm{d}s'. \tag{13.7}$$

The Saffman and Taylor [1958] solutions are given by

$$q_0 = \sqrt{\frac{1-s}{1+\alpha s}} \tag{13.8a}$$

$$\theta_0 = \cos^{-1} q_0, \tag{13.8b}$$

where

$$\alpha = \frac{2\lambda - 1}{(1-\lambda)^2}. \tag{13.9}$$

See further notes.[1]

[1] In his PhD thesis, McLean derives the (q, θ) leading-order solution directly from the Saffman-Taylor (x, y) solution in (13.2), then also demonstrates from direct substitution into the governing equations that it satisfies the equations; it is not made precisely clear how easy it is to derive the above without access to the Fourier-series summed solutions of Saffman and Taylor.

13.3 NUMERICAL SOLUTIONS AND THE LEADING-ORDER APPROXIMATION

We shall give a flavour of how the boundary integral formulation is numerically solved, and the resultant eigenvalues.

13.4 EXTENSION INTO THE COMPLEX PLANE

The leading-order solution (13.8a) contains a singularity in complex s-space, at $s = -1/\alpha$. Like the many examples of exponential asymptotics we have examined thus far, this singularity is expected to drive the divergence of the late terms. We will be required to study the behaviour of the asymptotic approximations for general complex values of s off the physical free-surface. Thus in preparation, we shall consider the extension of the governing system of equations (13.4) into complex values of s. This procedure is similar to the one in section 12.4.

The dynamic boundary condition (13.4b) needs no change, except now the differentiation is considered for complex s. The boundary integral equation (13.4a) can be extended into the complex plane by considering

$$\log q = -\frac{s}{\pi} \int_0^1 \frac{\theta(s')}{s'(s'-s)} \, \mathrm{d}s' + \mathrm{i}\theta(s), \tag{13.10}$$

where above, s is now a complex number in the upper-half plane[2]. Therefore, in order to obtain the analytic extension of $q(s)$ and $\theta(s)$ off the half finger, we use the complexified boundary integral equation (13.10) along with the dynamic condition (13.4b). Then the task will be to study the asymptotic expansion of the solutions.

[2] By taking s down to the axis along $0 < s < 1$, we can verify that the regular contour integral reduces to a principal-value integral plus half-a-residue contribution. Thus the integral $-\frac{s}{\pi}\int_0^1 \frac{\theta(s')}{s'(s'-s)}\,\mathrm{d}s'$ becomes $-\frac{s}{\pi}\fint_0^1 \frac{\theta(s')}{s'(s'-s)}\,\mathrm{d}s' - \mathrm{i}\theta(s)$.

As in Chapman [1999], it is useful to consider an additional transformation that maps the slit s-plane to a more convenient domain, particularly due to the fact that the top- and bottom of the fingers map to the top- and bottom of the slit $0 < s < 1$. Setting

$$y = -\sqrt{\frac{1-s}{s}}, \tag{13.11}$$

the free surface now lies entirely on the real y-axis, with the symmetry axis about the origin. Take care to note that the y used henceforth is not the vertical physical coordinate. The y-plane is shown in fig. 13.6.

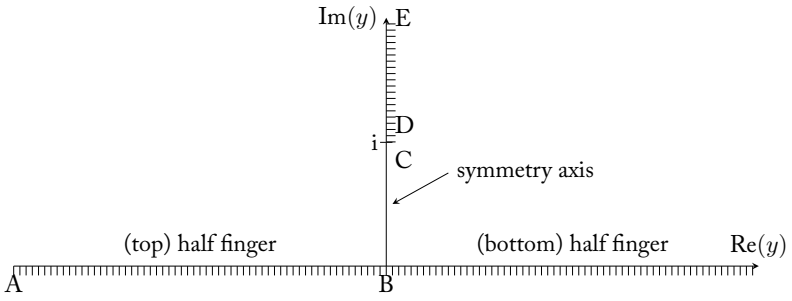

Figure 13.6: Configuration in the y-plane.

The set of equations is now

$$\log q - \mathrm{i}\theta = \hat{\mathscr{H}}[\theta](y), \tag{13.12a}$$

$$\epsilon^2 \frac{q(1+y^2)}{4y} \frac{\mathrm{d}}{\mathrm{d}y}\left(\frac{q(1+y^2)}{y}\frac{\mathrm{d}\theta}{\mathrm{d}y}\right) - q = -\cos\theta, \tag{13.12b}$$

$$\theta(-\infty) = 0, \tag{13.12c}$$

$$\theta(0) = -\frac{\pi}{2}.$$

Note that under this coordinate change and the symmetry axis, we may now replace the condition at the origin with the condition that

$$\theta(\infty) = -\pi. \tag{13.12d}$$

Above, we have defined the (complex) Hilbert transform, $\hat{\mathscr{H}}$, of a function to be

$$\hat{\mathscr{H}}[\theta](y) = \frac{2}{\pi}\int_{-\infty}^{0} \frac{y'\theta(y')}{y^2 - y'^2}\,\mathrm{d}y'. \tag{13.13}$$

Note that this definition of $\hat{\mathscr{H}}$ differs from that introduced in chapter 12.

13.5 EXPONENTIAL ASYMPTOTICS

The strategy for application of exponential asymptotics to the viscous fingering problem will be similar to the case of free-surface flow in chapter 12. We begin by naively expanding the solution as a perturbative series

$$q = \sum_{n=0}^{\infty} \epsilon^{2n} q_n \quad \text{and} \quad \theta = \sum_{n=0}^{\infty} \epsilon^{2n}\theta_n, \tag{13.14}$$

and seek to establish the eventual divergence of the asymptotic expansion after studying a number of the low-order terms. The integro-differential form of the system (13.12), which involves an integral of the solution along the boundary, poses some challenge. However, like for the case of low-Froude water waves in chapter 12, there is a critical argument (in section 13.5.1) that essentially allows the boundary-integral term to be neglected when consider the late terms of the asymptotic expansion.

At $\mathcal{O}(1)$, the solution is given by solving

$$\log q_0 - \mathrm{i}\theta_0 = \hat{\mathscr{H}}\theta_0, \tag{13.15a}$$

$$q_0 = \cos\theta_0, \tag{13.15b}$$

$$\theta_0(-\infty) = 0, \qquad \theta_0(\infty) = -\pi. \tag{13.15c}$$

The solution is the Saffman-Taylor solution[3] (13.8), which is given in the new notation as

$$q_0 = \cos\theta_0 = -\frac{y}{(1+\alpha+y^2)^{1/2}}, \tag{13.16a}$$

$$\sin\theta_0 = -\frac{(1+\alpha)^{1/2}}{(1+\alpha+y^2)^{1/2}}, \tag{13.16b}$$

where $\alpha = \alpha(\lambda)$ is defined by (13.9) and relates to the non-dimensional finger width λ. Notice that the leading-order asymptotic solutions, q_0 and θ_0, contain singularities[4] in the complex plane at $y = \pm \mathrm{i}\sqrt{1+\alpha}$, and there are further potential singularities at $y = 0$ and $y = \pm 1$ on account of the differential equation (13.12b).

In the limit $n \to \infty$, we posit the factorial-over-power ansatz,

$$q_n \sim \frac{Q(y)\Gamma(2n+\gamma)}{[\chi(y)]^{2n+\gamma}} \qquad \theta_n \sim \frac{\Theta(y)\Gamma(2n+\gamma)}{[\chi(y)]^{2n+\gamma}} \tag{13.17}$$

In fact, only the ansatz for θ_n is required as there is an expression [cf. later (13.19)] that relates θ_n with q_n.

13.5.1 Subdominance of the boundary integral

Let us first turn to the boundary integral equation (13.12a) and seek the $\mathcal{O}(\epsilon^{2n})$ terms. Expanding the full logarithm, for instance, produces,

$$\begin{aligned}\log q &= \log q_0 + \log\left[1 + \left(\epsilon^2\frac{q_1}{q_0} + \ldots\right)\right] \\ &= \log q_0 + \left[\left(\epsilon^2\frac{q_0}{q_0} + \ldots + \epsilon^{2n}\frac{q_n}{q_0} + \ldots\right) - \frac{1}{2}\left(\epsilon^2\frac{q_0}{q_0} + \ldots + \epsilon^{2n}\frac{q_n}{q_0} + \ldots\right)^2 + \ldots\right].\end{aligned}$$

As usual, the nonlinearity of the quantities renders extraction of the orders difficult. However, in considering (13.12a) we do not need the full list of terms at $\mathcal{O}(\epsilon^{2n})$, only

$$\left[\frac{q_n}{q_0} + \mathcal{O}(q_{n-1})\right] - \mathrm{i}\theta_n = \hat{\mathscr{H}}\theta_n. \tag{13.18}$$

Notice here that we have not included terms that are factors of q_{n-1}, q_{n-2}, and so forth. In essence, these terms are sufficiently subdominant as $n \to \infty$ and are not required in order to characterise the leading-order divergence.

At this point, there is a trick that allows us to argue the subdominance of the Hilbert transform term $\hat{\mathscr{H}}\theta_n$ as $n \to \infty$. Observe that this term is given by

$$\hat{\mathscr{H}}\theta_n = \int_{-\infty}^{0} \frac{\bar{y}\theta_n(\bar{y})}{y^2 - \bar{y}^2}\,\mathrm{d}\bar{y}.$$

Thus, in following the procedure, we would typically substitute the ansatz (13.17) into the above transform and estimate the size of the resultant integral. However, notice that the above integral the late terms

[3] Please insert more details to derive!

[4] Taking the arcsin for θ_0 also yields a (removable?) singularity where $\sin\theta_0 = \pm 1$ or $y = 0$. Might need to have a think about whether this has an effect?

Note that this compares with Chapman [1999] eqn (3.12) who uses the ansatz for θ_n of $\Lambda\Gamma(2n+\gamma_C+1)/[u(y)]^{2n+\beta(y)}$. We can transform our (13.17) to this alternative ansatz by setting $\gamma = \gamma_C + 1 =$, $\Theta = \Lambda/u^{\beta-\gamma}$ and $\chi = u$. Our choice allows consistency throughout this book.

along the negative $\bar{y}$-axis, and hence its magnitude is approximately controlled by the smallest values of χ along the axis. Once we have found χ through the procedure in the next section, we can verify *a posteriori* that the dominant contribution to the integral comes from the endpoint $\bar{y} = 0$ and that this contribution is subdominant to the terms on the left hand-side of (13.18) for those regions of $y \in \mathbb{C}$ which we are concerned. Thus we have a reduction of the boundary-integral equation to

$$q_n \sim \mathrm{i} q_0 \theta_n \quad \text{as } n \to \infty. \tag{13.19}$$

The idea that the Hilbert transform can be largely neglected in the analysis of the late terms is a significant simplification, and the consequence is that the exponential asymptotics analysis then resembles those typical cases of nonlinear differential equations presented earlier. For the case of the Saffman-Taylor viscous fingering problem, the legitimacy of the manipulation was proved rigorously by Tanveer and Xie [2003] but it was used in a somewhat ad-hoc manner those who first solved the viscous fingering problem.

13.5.2 Late orders analysis of the surface equation

We now turn to analysis of the $\mathcal{O}(\epsilon^{2n})$ terms of Bernoulli's equation (13.12b). In expanding this expression under the series substitution, we essentially seek to determine the two highest orders as $n \to \infty$ since these are involved in determining the values of χ and Θ. Here, terms like θ_n will dominate terms such as θ_{n-1} since each downwards shift of the subscript corresponds to a subtraction in the argument of the Gamma function (and hence slower growth in n). Similarly, differentiation of a term, say θ_n, increases the order in comparison with the undifferentiated term on account of the power in the denominator of ansatz (13.17). There is thus an equivalency between differentiation and shifting of the indices. [5]

[5] By the nature of the factorial-over-power expansion, two derivatives will be equivalent to substituting $n \to n+1$ in the order. It will turn out that we need to keep terms that include θ''_{n-1}, $\{\theta'_{n-1}, q'_{n-1}\}$, and θ_n.

We have that at $\mathcal{O}(\epsilon^{2n})$ for $n \geq 1$,

$$\frac{q_0(1+y^2)}{4y}\frac{\mathrm{d}}{\mathrm{d}y}\left[\frac{q_{n-1}(1+y^2)}{y}\theta_0'\right] + \frac{q_{n-1}(1+y^2)}{4y}\frac{\mathrm{d}}{\mathrm{d}y}\left[\frac{q_0(1+y^2)}{y}\theta_0'\right] + \frac{q_0(1+y^2)}{4y}\frac{\mathrm{d}}{\mathrm{d}y}\left[\frac{q_0(1+y^2)}{y}\theta_{n-1}'\right] + \ldots - q_n = \theta_n \sin\theta_0 + \ldots$$

We can simplify this expression by setting

$$P(y) = \frac{1+y^2}{y^2}. \tag{13.20}$$

Then expanding the derivatives and keeping relevant terms, we have

$$\left[\frac{q_0}{4}P^2\theta_0'\right]q_{n-1}' + \left[\frac{q_0^2}{4}P^2\right]\theta_{n-1}'' + \left[\frac{q_0}{4}P\frac{\mathrm{d}(q_0P)}{\mathrm{d}y}\right]\theta_{n-1}' + \ldots - q_n = \theta_n \sin\theta_0 + \ldots$$

Writing $q_n \sim \mathrm{i} q_0 \theta_n$ from (13.19) gives

$$\left[\frac{q_0^2}{4}P^2\right]\frac{\theta_{n-1}''}{\theta_n} + \left[\frac{\mathrm{i}q_0^2}{4}P^2\theta_0' + \frac{q_0}{4}P(q_0P)'\right]\frac{\theta_{n-1}'}{\theta_n} \sim \sin\theta_0 + \mathrm{i}q_0. \tag{13.21}$$

We now substitute the ansatz (13.17) and expand the ratios. [6] Collecting terms at $\mathcal{O}(1)$ and $\mathcal{O}(1/n)$ yields respectively:

$$\left[\frac{q_0^2}{4}P^2\right](\chi')^2 = \sin\theta_0 + \mathrm{i}q_0, \tag{13.22}$$

$$\frac{\Theta'}{\Theta} = -\frac{1}{2}\left[\frac{\chi''}{\chi'} + \mathrm{i}\theta_0' + \frac{(q_0P)'}{q_0P}\right]. \tag{13.23}$$

The first equation yields the singulant function, χ, and is discussed in the next section. The second equation yields the pre-factor function; it is integrated directly to obtain

$$\Theta(y) = \frac{\Lambda \mathrm{e}^{-\mathrm{i}\theta_0(y)/2}}{[\chi'(y)q_0(y)P(y)]^{1/2}}, \tag{13.24}$$

where Λ is a constant of integration determined from a later inner-matching procedure. At this point, recall that we have derived the components $\Theta(y)$ and $\chi(y)$ appearing in the late-orders ansatz (13.17). Moreover, one Θ has been determined, then Q follows from the relationship of (13.19) and hence

$$Q(y) = \mathrm{i}q_0(y)\Theta(y). \tag{13.25}$$

Thus, we only have the constants γ and Λ to be determined in order to fully characterise the divergence of the asymptotic expansions. Before deriving these constants, which are determined using a matched asymptotics expansion near the relevant singularities, let us study the crucial function χ.

[6] From the late-orders ansatz and the expansion of the Gamma function, we have the ratio of

$$\frac{\theta'_{n-1}}{\theta_n} = \frac{1}{2n}\left[-\chi'\chi\right] + \dots$$

for the first derivative term. Similarly, the second-derivative term yields the ratio of

$$\frac{\theta''_{n-1}}{\theta_n} = (\chi')^2 + \frac{1}{2n}\left[-2\chi'\chi\frac{\Theta'}{\Theta} - \chi''\chi\right] + \dots$$

13.6 ANALYSIS OF THE SINGULANT

The singulant function, χ, given by solving (13.22) provides the key component of the viscous fingering selection mechanism. Solving for χ yields a choice of two square-root branches, $\pm$, as well as a constant of integration. Recall in our discussion in the paragraph above (13.17) that the singularities in the low-order terms, notably at

$$y = \pm\mathrm{i}\sqrt{1+\alpha}, \tag{13.26}$$

serve as the dominant mechanism producing divergence. By assumption of the asymptotic divergence, $\chi = 0$, at a selected singularity. Let us consider the nearest singularity in the upper half-plane, located at $y = \mathrm{i}(1+\alpha)^{1/2}$. Then the corresponding singulant function is[7]

$$\chi(y) = 2\mathrm{i}\int_{\mathrm{i}(1+\alpha)^{1/2}}^{y} \frac{[(1+\alpha)^{1/2} + \mathrm{i}\bar{y}]^{3/4}[(1+\alpha)^{1/2} - \mathrm{i}\bar{y}]^{1/4}}{1+\bar{y}^2}\,\mathrm{d}\bar{y}. \tag{13.27}$$

As is typical by this stage of our work, Stokes line are expected along those curves, such that

$$\operatorname{Im}\chi(y) = 0 \quad \text{and} \quad \operatorname{Re}\chi(y) \geq 0.$$

across which an exponentially-small term is expected to be switched on. In fact, the integral (13.27) can be explicitly integrated (but otherwise,

[7] In general, there is a singulant function produced for each singularity in the analytic continuation of the low-order asymptotic terms—that is, for a general point $y \in \mathbb{C}$, the divergence of the asymptotic expansion is dominated by a factorial-over-power growth with a singulant function that has the smallest value of $|\chi|$ at that point. However, we are firstly considering the divergence at a point y along the real axis.

contours can be calculated by numerical quadrature) and the Stokes lines visualised in the complex y-plane.

Consider firstly the case of $\alpha < 0$. This produces a Stokes line configuration of fig. 13.7. In this case, there is a central Stokes line that switches on terms across the origin, $y = 0$. These terms cannot be switched off. In particular, the symmetry condition at $y = 0$ cannot be satisfied and is off by an exponentially small error. We thus argue that for $\alpha < 0$, solutions do not exist in the limit $\epsilon \to 0$.

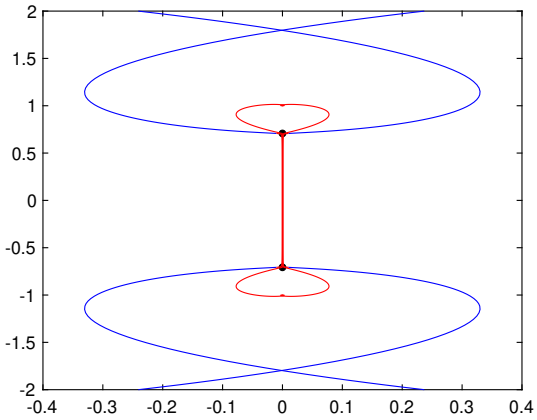

Figure 13.7: Stokes lines for the case of $\alpha = -0.5$. NB: these are actually equal phase lines and I have not yet removed curves with $\mathrm{Re}\,\chi < 0$.

In contrast, for the case of $\alpha > 0$, the Stokes lines shown in fig. 13.8 show that there is now a localised region near the origin where exponentials can be switched on, firstly for $y < 0$, but then switched off for $y > 0$. In order for this to occur, we must ensure that ϵ is 'tuned' appropriately for the size of the localised region between Stokes lines.

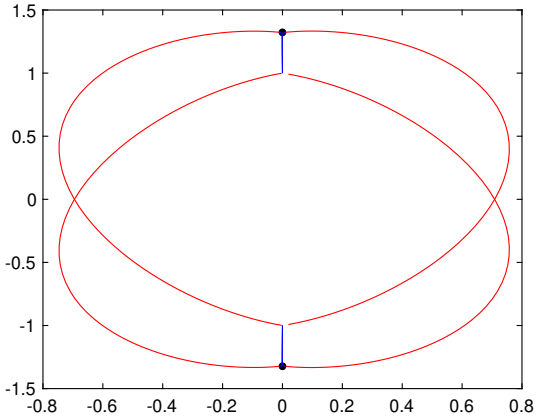

Figure 13.8: Stokes lines for the case of $\alpha = 0.75$. The singularity at $y = \mathrm{i}\sqrt{1+\alpha}$ produces two relevant Stokes lines that curve downwards. Similarly, the mirror singularity in the lower half-plane produces two Stokes linse curving upwards. A localised region is produced where oscillations must be contained.

The Stokes line arrangement for the case of $\alpha > 0$ also shows a possible distinguished limit. If $\alpha \to 0$ simultaneously to $\epsilon \to 0$, then the singularity at $y = \mathrm{i}\sqrt{1+\alpha}$ merges with he singularity at $y = \mathrm{i}$, and we can no longer assume that the Stokes contributions are non-interacting and additive. The analysis of this distinguished limit, which happens to be for $\alpha = \mathcal{O}(\epsilon^{4/3})$, demands a separate investigation.

13.7 OPTIMAL TRUNCATION AND STOKES SWITCHING

Details to be included...

The Stokes line switching should be very similar to the case of low-Froude flows, and we would expect that across Stokes lines, an exponential scaling like

$$q_{\text{exp}} \sim \text{const.} \times Q(y)\mathrm{e}^{-\chi(y)/\epsilon}. \tag{13.28}$$

Complex conjugate contributions are also switched on.

We can either impose the dual-wave constraint or instead impose a zero first derivative at the origin.

13.8 VARIATIONS

Kinetic undercooling Chapman and King [2003]

13.9 EXERCISES

1. Derive the Saffman-Taylor zero-surface-tension solution in (13.2). This follows the derivation shown in Saffman and Taylor [1958], p. 351 by expressing y as a Fourier series,

$$y = \frac{\psi}{V} + \sum_{n=1}^{\infty} A_n \sin\left(\frac{n\pi\psi}{V}\right) \mathrm{e}^{-n\pi/\phi/V}. \tag{13.29}$$